DOI: 10.1002/cbic.200800282

Design of Gold Nanoparticle-Based Colorimetric Biosensing Assays

Weian Zhao,[a] Michael A. Brook,*[a] and Yingfu Li*[a, b]

Gold nanoparticle (AuNP)-based colorimetric biosensing assays have recently attracted considerable attention in diagnostic applications due to their simplicity and versatility. This Minireview summarizes recent advances in this field and attempts to provide general guidance on how to design such assays. The key to the AuNP-based colorimetric sensing platform is the control of colloidal AuNP dispersion and aggregation stages by using biological processes (or analytes) of interest. The ability to balance interparticle attractive and repulsive forces, which determine whether AuNPs are stabilized or aggregated and, consequently, the color of the solution, is central in the design of such systems. AuNP aggregation in these assays can be induced by an "interparticle-crosslinking" mechanism in which the enthalpic benefits of interparticle bonding formation overcome interparticle repulsive forces. Alternatively, AuNP aggregation can be guided by the controlled loss of colloidal stability in a "noncrosslinking-aggregation" mechanism. In this case, as a consequence of changes in surface properties, the van der Waals attractive forces overcome interparticle repulsive forces. Using representative examples we illustrate the general strategies that are commonly used to control AuNP aggregation and dispersion in AuNP-based colorimetric assays. Understanding the factors that play important roles in such systems will not only provide guidance in designing AuNP-based colorimetric assays, but also facilitate research that exploits these principles in such areas as nanoassembly, biosciences and colloid and polymer sciences.

1. Introduction

The controlled assembly and disassembly of gold nanoparticles (AuNPs) has been a subject of great interest over the past decade due to the potential applications of these particles in nanobiotechnology.[1] Their unique physical properties,[2] particularly their localized surface plasmon resonance (LSPR; section 2), make AuNPs attractive building blocks for nanoscale electronic and photonic devices as well as signal transducers and/or signal amplifiers in a variety of biosensing platforms that exploit colorimetric (through interparticle plasmon coupling or local refractive index change-induced plasmon band shifts),[3a] plasmonic light scattering,[3b] surface-enhanced Raman scattering (SERS),[3c–e] fluorescent,[3f–h] and electrochemical assays.[3i–k]

Of particular interest is the AuNP-based colorimetric biosensor, which takes advantage of the color change that arises from the interparticle plasmon coupling during AuNP aggregation (red-to-purple or blue) or redispersion of an AuNP aggregate (purple-to-red).[1a,b,4] Since the first DNA sensor was developed by Mirkin and co-workers,[5] this platform has been increasingly applied for the detection of a large variety of targets, (Tables 1 and 2) including nucleic acids, proteins, saccharides, small molecules, metal ions, and even cells. It is quickly becoming an important alternative to conventional detection techniques (e.g., fluorescence-based assays) and holds great potential in clinical diagnostics, drug discovery, and environmental contaminant analysis, among others.

In this Minireview, we attempt to summarize the recent advances in the development of AuNP-based colorimetric biosensing assays that employ AuNP aggregation and dispersion. Given that excellent, but general, review articles for some relevant topics on AuNPs exist (the preparation, surface functionalization, physical properties, applications including biosensing platforms other than absorption-based colorimetric assays,[1a,b,2,6] biomolecule-mediated nanoassembly,[1d–l] DNA nanotechnology,[7] and nanoparticle-based bioanalysis[8]), we will address the subject from the standpoint of colloid chemistry and attempt to provide general guidelines on how to design AuNP-based colorimetric biosensors by tuning interparticle forces and controlling AuNP colloidal stability and aggregation. We begin with a brief introduction of the physical phenomenon (i.e., colors) associated with AuNPs and their aggregation, briefly discuss the interparticle forces of AuNPs, and describe general strategies to stabilize or aggregate these colloidal particles. After providing a general background, we will concentrate on the design of biosensing assays through the modulation of AuNP stability and aggregation, which utilize both interparticle crosslinking and noncrosslinking aggregation mechanisms.

[a] *W. Zhao, Prof. Dr. M. A. Brook, Prof. Dr. Y. Li*
Department of Chemistry, McMaster University
1280 Main Street, W. Hamilton, ON L8S 4M1 (Canada)
Fax: (+1) 905-522-9033
E-mail: liying@mcmaster.ca
mabrook@mcmaster.ca

[b] *Prof. Dr. Y. Li*
Department of Biochemistry and Biomedical Sciences
McMaster University, 1280 Main Street
W. Hamilton, ON, L8N 3Z5 (Canada)

Table 1. Typical types of interparticle (bio)recognitions and their representative target analytes in AuNP-based colorimetric biosensing assays by using the interparticle crosslinking aggregation mechanism. See Figure 3 and the main text for a detailed description of each platform.

Platform	Interparticle biorecognition						
	DNA–DNA	aptamer–target	antibody–antigen	streptavidin–biotin	lectin–sugar	metal–ligand	other chemical interactions[a]
A	nucleic acids,[5,14t] DNA binding molecules,[13,14s] Hg^{2+},[13c,14k] proteins,[14r] cysteine,[13a] cytokine[14v]	thrombin,[14a] cells,[14j] PDGF,[14b] ATP,[14c]	antibody[14d,f]	streptavidin[14e]	lectin,[14o,p] cholera toxin[14h]	heavy metals,[14i] Cu^{2+},[14u] K^{+}[14g]	cysteine and glutathione,[14q] phage[14m]
B	Pb^{2+}, adenosine, cocaine[15]			biotin[20c]	glucose,[16] protein–protein interaction[17]		
C	Pb^{2+},[18f] K^{+},[14c] adenosine,[18g] Cu^{2+}[14c]						protease,[18a] β-lactamase,[18d] phosphatase,[14c] H_2O_2,[18c] protein modification[18e]
D	kinase[19a]			streptavidin[14n]			
E	DNase I[20a]						protease[20b]
F	pH[19c,d,14l]			kinase[19a]			cytochrome c[19b]

[a] These include AuNP crosslinking with molecules that bear multiple AuNP surface binding sites (e.g., thiol) through chemical interactions (e.g., Au–S).

Table 2. Typical platforms and their representative target analytes in AuNP-based colorimetric biosensing assays using the noncrosslinking aggregation mechanism. See Figure 4 and the main text for a detailed description of each platform.

Platforms	G	H	I
targets	DNA,[22a] K^{+},[22d] ATP,[22f] thrombin,[22e] kinase,[22g,h] Hg^{2+},[22j] lysozyme,[22i] phosphatase[11]	adenosine,[23a] DNase I,[23b] Pb^{2+},[23b] nucleic acids[31]	DNA,[21] adenosine,[12] adenosine deaminase,[12] K^{+}[12]

2. Localized Surface Plasmon Resonance of AuNPs

Small AuNPs (normally 10–50 nm in diameter) in water or glass appear deep-red in color, a phenomenon that has fascinated people since ancient Roman times. The physical origin of this phenomenon is associated with the coherent oscillation of AuNP surface electrons (localized surface plasmon) induced by the incident electromagnetic field.[1a,b] When visible light shines on AuNPs, the light of a resonant wavelength is absorbed by AuNPs and induces surface electron oscillation. Small AuNPs (e.g., 13 nm in diameter) absorb green light, which corresponds to a strong absorption band (surface plasmon band) at ~520 nm in the visible light spectrum; therefore solutions of AuNPs appear red in color (Figure 1B, red line). For small AuNPs, surface electrons are oscillated by the incoming light in a dipole mode. As the size of the AuNP increases, light can no longer polarize the nanoparticles homogeneously, and higher order modes at lower energy dominate. This causes a red-shift and broadening of the surface plasmon band.[1a] This also explains the corresponding surface plasmon band shifts (red-shift) and color changes (red-to-purple) that are observed during the aggregation of small AuNPs (Figure 1B, blue line). When AuNPs aggregate, their surface plasmons combine (interparticle plasmon coupling), and the aggregate could be considered as a single large particle, although the detailed interparticle plasmon coupling is rather complex and dependent on many factors, such as aggregate morphology and nanoparticle density.[1a] For the detailed physics of LSPR and interparticle plasmon coupling, which is beyond the scope of this Minireview, we recommend some excellent review articles, such as refs. [1a,b,2].

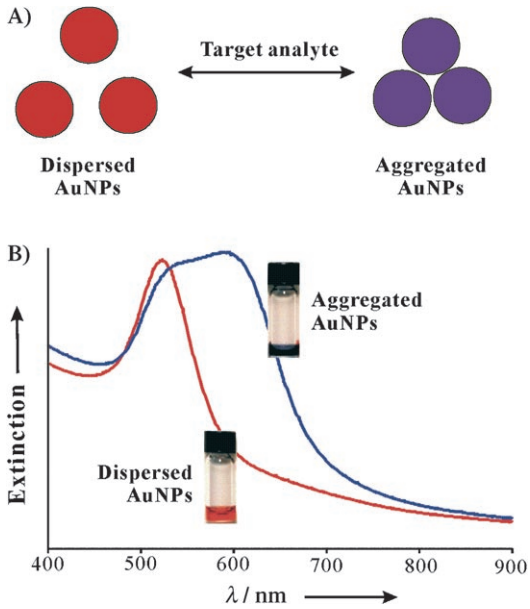

Figure 1. A) General schematic representation of absorption-based colorimetric AuNP biosensing assays by using AuNP aggregation and dispersion. B) Typical surface plasmon absorption bands for 13 nm AuNPs in the visible light region. The red and blue curves correspond to dispersed and aggregated AuNPs, respectively.

It is the predictable color change during AuNP aggregation (or redispersion of an aggregate) that provides an elegant platform for absorption-based colorimetric detection with AuNPs

as signal reporters.[5] A target analyte or a biological process that directly or indirectly triggers AuNP aggregation (or redispersion of an aggregate) can be detected by the color change of the AuNP solution (Figure 1 A). As interparticle plasmon coupling can generate a huge absorption band shift (up to ~300 nm), the color change can be observed by the naked eye, and therefore sophisticated instruments are not required for qualitative analysis. Importantly, owing to their extremely high extinction coefficients (e.g., $2.7\times10^8\,\text{M}^{-1}\,\text{cm}^{-1}$ at ~520 nm for 13 nm spherical AuNPs, ≥1000 times higher than those of organic dyes),[1a] AuNP-based colorimetric assays have high sensitivity, which is comparable to that of conventional biodetection assays that, for example, use fluorescence.[1a,b] For quantitative analysis, the absorption spectra are recorded (normally at an arbitrarily chosen assay time, given the fact that AuNP aggregation is a continuous process) by using a standard spectrophotometer (Figure 1 B). The ratio of the absorbances at 520 nm, which corresponds to dispersed particles, and a longer wavelength (e.g., 600 nm) for a given system, which corresponds to aggregated particles, is often used to quantify the aggregation process or color change. Sometimes, an aggregation parameter, which measures the variation of the integrated absorbance between, for example, 600 and 700 nm, is used for quantitative analysis, and this method can provide a higher sensitivity.[3l] Typically, the detection limit of current AuNP-based colorimetric assays, without signal amplification steps, is in the range of nM to μM—depending on both the design of the system (sections 4 and 5) and the binding affinity of the biomolecule receptor used in the assay.

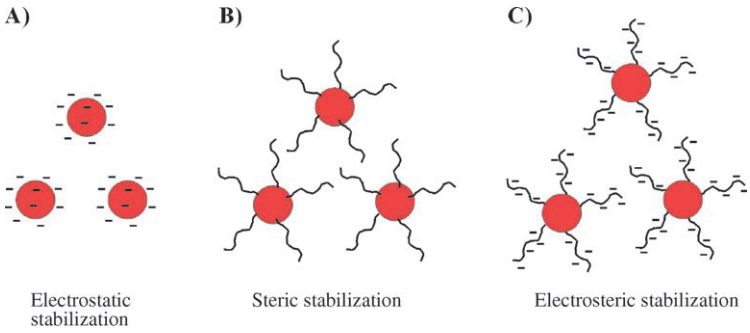

Figure 2. Schematic representation of colloidal stabilization through A) small charged molecules on the AuNP surface (electrostatic stabilization), B) surface grafted polymers (steric stabilization), and C) surface grafted charged polymers (electrosteric stabilization).[9]

3. Colloidal AuNP Stabilization

The key to the AuNP-based colorimetric sensing platform is the control of the colloidal AuNP dispersion and aggregation stages with a biological process (or analyte) of interest. AuNP stabilization or aggregation depends on the net potential between interparticle attractive and repulsive forces.[9]

AuNPs after preparation are often stabilized against van der Waals attraction-induced aggregation by surface-tethered capping ligands—species used to control AuNP growth in the AuNP preparation process. For instance, AuNPs prepared by the classic citrate reduction method[10] are stabilized in water by charged citrate ions on their surface. The stability of AuNPs can be further controlled to an exceptional degree through the introduction of colloidal stabilizers (see below) by using chemical grafting methods (e.g., Au–thiol, Au–amine), electrostatic adsorption and physical adsorption, etc. Common colloidal stabilizers include charged small molecules, polymers, and polyelectrolytes, which stabilize the colloidal particles through electrostatic, steric, and electrosteric (a combination of electrostatic and steric) interactions, respectively (Figure 2).[9]

With respect to electrostatic stabilization (Figure 2 A), the surface charges, together with the counter ions in the medium, form a repulsive electric double layer that stabilizes colloids against van der Waals attractive forces.[9c,d] A characteristic feature of electrostatic repulsion is its high sensitivity to the bulk ionic strength; the force of electrostatic repulsion diminishes significantly at high salt concentrations, when the electric double layer is highly suppressed.[9c,d] This explains why citrate-capped AuNPs are stabilized in water but undergo aggregation at elevated salt concentrations (e.g., 50 mM NaCl).[11]

In the case of steric stabilization[9a,e,f] (Figure 2 B), macromolecules grafted on colloid surfaces in a "good solvent"—that is, a solvent in which steric stabilization diminishes with decreasing solubility—impart a polymeric barrier that prevents colloids from coming too close, and van der Waals attractive forces can dominate.[9a,e,f] Essentially, the penetration of polymer chains on colloids when they approach each other results in a loss of polymer configurational entropy, which disfavors the aggregation process.[9a,e,f] Steric stabilization is much less sensitive towards ionic strength than electrostatic stabilization. Rather, the molecular weight of the macromolecule and surface graft density are more important factors. In general, thicker polymer layers and higher graft densities lead to more effective steric stabilization.[9a,e,f]

Electrosteric stabilization provided by surface-tethered charged polymers (Figure 2 C) is probably the most effective strategy to stabilize colloidal particles.[9a,e,f] DNA (negatively charged polymer) modified AuNPs represent an excellent example of such systems. DNA-modified AuNPs with high DNA graft density remain stabilized even at very high salt concentrations (e.g., 300 mM $MgCl_2$). Steric factors are expected to play a major role in stabilizing AuNPs at salt concentrations in which the electrostatic repulsion is significantly diminished.[12]

4. Interparticle Crosslinking Aggregation

The controlled aggregation of AuNPs in absorption-based colorimetric biosensing assays can be realized by interparticle bonding formation (interparticle crosslinking aggregation mechanism) or by the removal of colloidal stabilization effects (noncrosslinking aggregation mechanism). Interparticle crosslinking aggregation is, so far, the most common approach through which AuNPs are brought together. This occurs either

by using crosslinker molecules that have multiple binding sites for the receptor molecules on AuNPs (Figure 3A), or by the direct interaction (without crosslinkers) between receptor-modified AuNPs and AuNPs to which complementary (or anti-receptor) molecules are attached (Figure 3B). In the case of interparticle crosslinking initiated aggregation, the enthalpic benefits of interparticle bond formation (e.g., H-bonding, electrostatic attraction, hydrophobic interaction, metal–ligand coordination) associated with interparticle biological recognition, overcome the interparticle repulsive forces (electrostatic and/or steric repulsion). Typical biological recognition events include DNA hybridization, aptamer–target interactions, antibody–antigen interactions, streptavidin–biotin interactions, lectin–sugar interactions, and metal–ligand coordination. Furthermore, biologically relevant organic molecules (such as peptides) that have multiple gold surface binding tags (such as thiol and guanidine) can also directly crosslink AuNPs by chemical interactions (e.g., Au–S). Table 1 summarizes the typical interparticle (bio)recognition mechanisms and their representative target analytes in AuNP-based colorimetric biosensing assays that use the interparticle crosslinking aggregation mechanism.

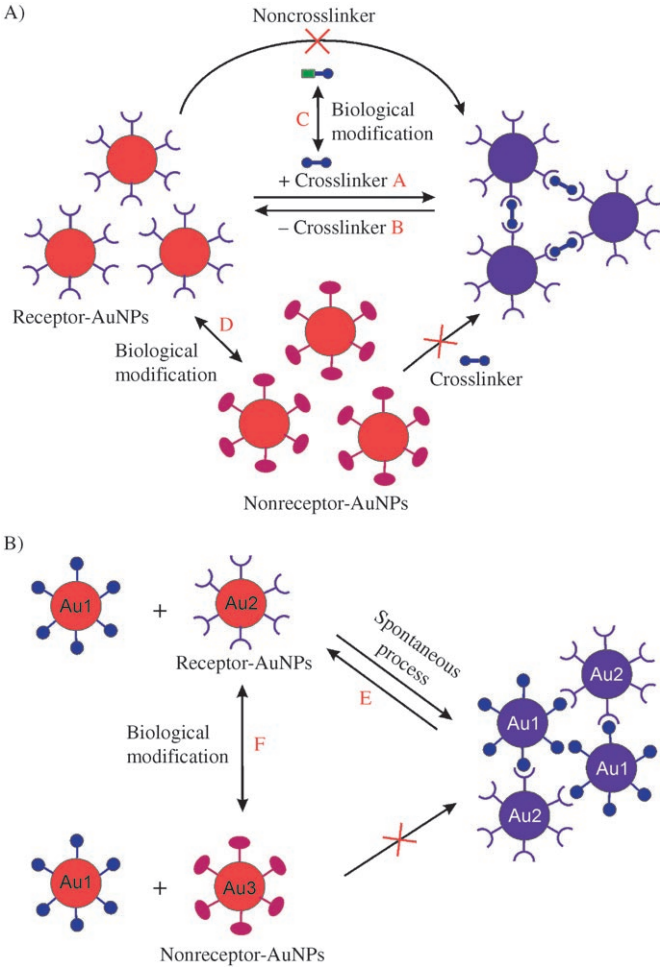

Figure 3. Interparticle crosslinking AuNP aggregation. A) AuNPs are brought together by crosslinking molecules that have multiple binding sites for the corresponding receptors on AuNPs (pathway A). Biological recognition events (or processes) that remove (or break) crosslinking molecules cause AuNP deaggregation (pathway B). Biological recognition events (or processes) that can modify crosslinking molecules (pathway C) or receptors on AuNP surface (pathway D) can indirectly control AuNP aggregation and deaggregation. B) AuNP aggregation is induced by direct recognition (without crosslinkers) of receptor-modified AuNPs and complementary (or anti-receptor) AuNPs. Biological recognition events (or processes) that break these interparticle interactions result in AuNP deaggregation (pathway E). The AuNP aggregation process can also be regulated by biological processes that modify surface-attached receptors (pathway F). See the main text for detailed description of different assay designs in pathways A–F.

The first and most popular platform detects a target analyte (crosslinker) that bears multiple binding sites for the receptors on AuNPs (Figure 3A, pathway A). A classic example is the DNA sensor developed by Mirkin and co-workers, in which target DNA molecules trigger AuNP aggregation by hybridizing two complementary DNA strands on AuNPs.[5] A red-to-purple color change is therefore observed upon the addition of target DNA. Given the nature of DNA hybridization, the aggregation process is fully reversible; denaturation of the hybridized DNA duplex at elevated temperature (above the melting temperature) causes the dissociation of aggregates into dispersed AuNPs. Remarkably, the melting transition is extremely sharp, which might enhance the selectivity of perfectly-matched target DNA strands over those with mismatches.[5] Using a similar strategy, Mirkin and colleagues have recently developed assays for the detection of DNA-binding molecules and metal ions (e.g., Hg^{2+}).[13] This platform (Figure 3A, pathway A) has also been applied by many others for the detection of a large variety of substances (Table 1).[14]

Due to the controllable reversibility of AuNP aggregation, one can also make purple-colored, crosslinked AuNP aggregates and then use them to detect analytes that dissociate the crosslinkers and redisperse the AuNP aggregates (Figure 3A, pathway B).[15–16] An inverse color change (purple-to-red) is anticipated in this case. Lu and co-workers have developed a series of such assays for the detection of Pb^{2+}, adenosine, and cocaine.[15] In the Pb^{2+}-sensing assay,[15a] for instance, DNA molecules with a single RNA linkage serve as crosslinkers that bring complementary DNA-attached AuNPs into aggregates. A DNA enzyme (DNAzyme) that is prehybridized with DNA substrate crosslinker cleaves the substrate by using Pb^{2+} as cofactor. Therefore, a purple-to-red color change indicates the presence of Pb^{2+}. Aslan et al. have applied a similar strategy for the detection of glucose.[16] In their assay, dextran modified AuNPs were aggregated by using concanavalin A (Con A) as crosslinker, which has multiple binding sites for dextran. The addition of glucose, which binds competitively to Con A, dissociates the AuNP aggregates into dispersed AuNPs, and leads to a purple-to-red color change. This type of competitive assay has also been used to study protein–protein interactions.[17]

Given that AuNP aggregation in the assays mentioned above is induced by the interaction of crosslinker and receptor molecules on AuNPs, biological processes that can convert the crosslinker molecules into noncrosslinker molecules (or vice versa; Figure 3A, pathway C)[18] or can modify receptor molecules into nonreceptor molecules (or vice versa; Figure 3A,

pathway D)[19] can therefore be indirectly detected. Representative examples regarding the modification of crosslinkers include protease detection assays, in which a protease digests a peptide crosslinker that would otherwise assemble AuNPs into aggregates.[18a] A similar strategy has also been applied for the detection of Pb^{2+}, β-lactamase, phosphatase, and hydrogen peroxide, among others.[18b–h] The assays that concern the modification of receptor molecules on AuNPs (Figure 3A, pathway D) will be discussed below together with pathway F in Figure 3B.

Interparticle crosslinking aggregation can also take place without crosslinkers (Figure 3B). If receptor molecule-modified AuNPs are mixed with another type of AuNPs to which complementary (or anti-receptor) molecules are attached, AuNPs spontaneously form aggregates through interparticle biorecognition (Figure 3B). This is the case when AuNP aggregates are prepared by mixing DNA-modified AuNPs with complementary DNA-tethered AuNPs.[20a] Mirkin and co-workers have prepared such purple-colored AuNP aggregates and used them as probes for the detection of endonuclease (DNase I) and its inhibitors (Figure 3B, pathway E).[20a] The addition of endonuclease cleaves double-stranded (ds) DNA strands and results in the dissociation of AuNPs, which is accompanied by a purple-to-red color change.

The detection of biological processes that modify biomolecule receptors on AuNP surfaces and lead to (or prevent) AuNP aggregation, is another common platform that uses the interparticle crosslinking aggregation mechanism with (Figure 3A, pathway D) or without crosslinker molecules (Figure 3B, pathway F).[19] Brust and co-workers reported a kinase-sensing assay in which a kinase catalyzes the phosphorylation of peptide substrates that are attached to AuNPs.[19a] As γ-biotin-ATP is used as a cosubstrate, the phosphorylation reaction introduces biotin onto AuNPs, which allows the kinase-modified AuNPs to crosslink with avidin-modified AuNPs and form aggregates through the interaction between avidin and biotin (Figure 3B, pathway F). A similar approach has also been applied to detect proteases, pH changes, and to study protein conformational changes.[19b–d]

In summary, AuNP-based colorimetric bioassays that employ an interparticle crosslinking aggregation mechanism rely on interparticle biorecognition forces (and sometimes chemical interactions). This aggregation mechanism is mainly applied to target biological processes (or analytes) that are directly or indirectly associated with the formation of interparticle bonds. One could readily design such systems, particularly for targets that have multiple binding sites on their receptors. On the other hand, however, this could restrict the use of such assays mainly to cases in which target analytes and/or receptors have multiple binding sites. Moreover, AuNP aggregation induced by interparticle crosslinking is sometimes a relatively slow process. For example, AuNP aggregation modulated by DNA hybridization between target DNA crosslinkers and DNA probes on AuNPs normally takes a few hours.[5] Careful annealing steps (heating and cooling) are often required in such systems. The relatively slow aggregation is presumably due to the nature of the interparticle crosslinking aggregation mechanism. Aggregation is mainly driven by random collisions between nanoparticles with relatively slow Brownian motion;[21a] additionally interparticle repulsive forces (electrostatic and/or steric) create high energy barriers for aggregation (although interparticle bonding formation is favored thermodynamically). Furthermore, when AuNP aggregates are used as probes (Figure 3, pathways B and E), biomolecules inside aggregates are only poorly accessible for biorecognition, which might impair both the detection sensitivity and assay time.[15]

5. Noncrosslinking Aggregation

More recently, a "noncrosslinking aggregation" or "destabilization-induced aggregation" mechanism has been employed as an alternative way to control AuNP aggregation in AuNP-based colorimetric biosensing assays. In such systems, AuNP aggregation is induced by the controlled loss of electrostatic, steric or electrosteric stabilizations without the formation of interparticle bonds (Figure 4, pathways G–I). Table 2 summarizes different sensing platforms that use the noncrosslinking aggregation mechanism and some representative target analytes.

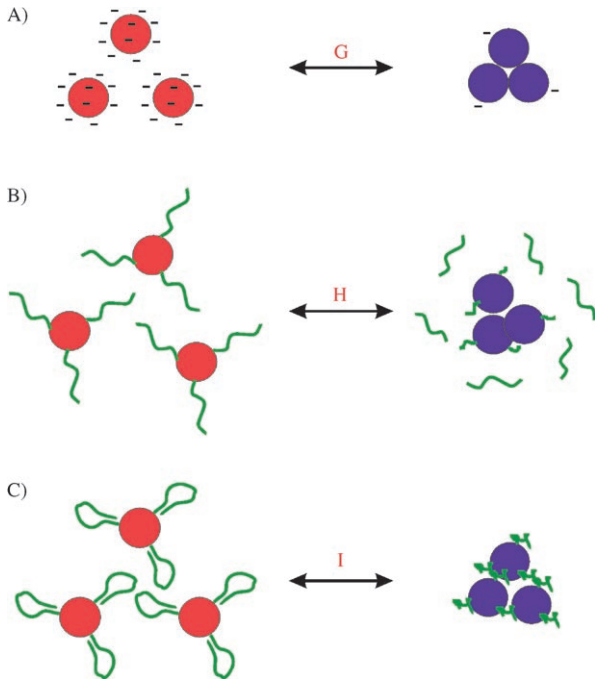

Figure 4. Representative strategies for the noncrosslinking aggregation mechanism. Van der Waals attractive forces dominate aggregation when interparticle repulsive forces are significantly reduced by A) the loss of electrostatic stabilization for small charged molecule-stabilized AuNPs. Representative examples are the use of AuNPs to monitor a biological reaction in which the reactant and product have different effects on AuNP surface charge properties, B) the loss of (electro)steric stabilization for (charged) polymer-stabilized AuNPs, such as the removal of DNA molecules from AuNPs by endonuclease cleavage, and C) (charged) polymer conformational transitions, such as DNA aptamer folding upon binding to its target. See the main text for a detailed description of pathways G–I.

5.1. Changing surface charge

AuNPs stabilized electrostatically by small charged moieties, such as citrate-capped AuNPs, undergo aggregation when surface charges are screened by the addition of salt, displaced by uncharged species or neutralized by oppositely-charged species (Figure 4A, pathway G). Citrate-capped AuNPs have been used for biodetection by using this principle.[11,22] For instance, Li and Rothberg found that single-stranded (ss) DNA can bind to citrate-capped AuNPs through DNA base–gold interactions and stabilize AuNPs electrostatically.[22a–c] In contrast, dsDNA formed by the hybridization of ssDNA and its complementary DNA target, shows little binding affinity to citrate-capped AuNPs and, therefore, it provides little stabilization, because, once hybridized, the DNA bases are not free to bind to AuNP surface. In other words, at an appropriate salt concentration (e.g., 200 mM NaCl), citrate-capped AuNPs are stabilized in the presence of ssDNA, but aggregate in the presence of dsDNA. This provides a means to detect the presence of target DNA or monitor DNA hybridization. A similar strategy has also been applied to the detection of K^+, thrombin and ATP, and takes advantage of the different effects of ssDNA aptamers with and without target analytes on citrate-capped AuNPs.[22d–f] More recently, using the same principle, Willner and co-workers have developed an ultrasensitive Hg^{2+} sensor in which thymine-rich nucleic acids affect AuNP stability differently in the presence and absence of Hg^{2+}.[22j]

We have expanded the use of this platform (pathway G) to the detection of enzymes or monitoring enzymatic reactions in which the reactant and product differently affect the surface charge properties of citrate-capped AuNPs.[11] In a dephosphorylation reaction, for example, ATP (reactant) is converted into adenosine (product) by alkaline phosphatase. ATP and adenosine both bind to the citrate-capped AuNP surface through DNA base–Au interactions, which presumably lead to the displacement of charged citrate ions from the AuNP surface. Therefore, the adsorption of highly charged ATP or uncharged adenosine either stabilizes AuNPs or causes their aggregation, respectively, due to the gain or loss of surface charges. Upon mixing citrate-capped AuNPs with the reaction solution at certain reaction times, the AuNP solution color, which corresponds directly to the amount of ATP and adenosine in the enzyme solution, reflects the degree of conversion of ATP to adenosine and indicates how far the enzyme-catalyzed reaction has proceeded.

Using a similar strategy, Oishi et al. have also developed assays for the detection of a protein kinase that phosphorylates a peptide substrate.[22g,h] They found that the nonphosphorylated peptide, which carries positive charges, can bind to the negatively charged citrate ion-capped AuNPs. The neutralization of surface charges in this case results in AuNP aggregation and a red-to-purple color change. In contrast, the phosphorylated peptide that has reduced positive charges did not cause AuNP aggregation.

5.2. Changing (electro)steric stabilization

5.2.1. Loss of polymeric stabilizers: A second platform that uses the noncrosslinking aggregation mechanism concerns (charged) polymer-modified AuNPs that are (electro)sterically stabilized (Figure 4B, pathway H). Biological processes (or analytes) that cause the loss of (electro)steric stabilization, for example, by removing (charged) polymers from AuNP surface, can be detected by using this platform. We have demonstrated an adenosine-sensing assay in which the addition of adenosine causes dissociation of DNA aptamers[24] (charged polymers) from the AuNP surface; this process results in AuNP aggregation at an appropriate salt concentration (e.g., 40 mM $MgCl_2$).[23a] We recently found that DNA molecules on AuNPs can also be removed by enzymatic cleavage using either a protein enzyme (DNase I) or a Pb^{2+}-mediated DNAzyme.[25] The resultant aggregation and red-to-purple color change indicate either the presence of DNase I or Pb^{2+}.[23b]

5.2.2. Structural changes of polymeric stabilizers: Another platform that employs a noncrosslinking aggregation mechanism relies on the change in colloidal AuNP stability upon (charged) polymer conformational transitions on the AuNP surface (Figure 4C, pathway I).[12,21] Maeda and co-workers discovered that AuNPs attached to ssDNA are more stable against salt-induced aggregation than dsDNA-tethered AuNPs formed by the hybridization of the complementary target DNA strand with DNA probes on AuNPs.[21a] The authors attribute this phenomenon to three factors: 1) the formation of a DNA duplex raises the binding constant with counter ions (e.g., Na^+) that screen the charges of DNA molecules on AuNPs, and therefore reduces the interparticle electrostatic repulsion;[21a] 2) the entropic loss associated with the formation of a rigid DNA duplex;[21a] and 3) interparticle DNA duplex association;[21c] in this case, the aggregation mechanism in this system becomes a different type of interparticle crosslinking mechanism (Figure 3B, pathway F).

We recently investigated DNA aptamer folding upon binding to a non-nucleic acid target molecule (adenosine or K^+) on the AuNP surface, and its effect on AuNP colloidal stability.[12] Interestingly, we observed a unique colloidal stabilization effect associated with aptamer folding; AuNPs attached to folded aptamer structures are more stable against salt-induced aggregation than those tethered to unfolded aptamers. Significantly, distinct AuNP aggregation and redispersion stages can be readily controlled by manipulating aptamer folding and unfolding states with adenosine and adenosine deaminase, respectively.[12] Our finding was initially a surprise, particularly when compared to the system described by Maeda and coworkers in which the formation of rigid DNA duplexes on AuNP surface resulted in colloidal destabilization. While the precise mechanism is not yet fully understood, the conformation that aptamers adopt on AuNP surfaces appears to be a key factor that determines the relative stabilities of different AuNPs.[12] Dynamic light scattering (DLS) experiments revealed that the height of the folded aptamer layer on AuNP surface was larger than that of the unfolded (but largely collapsed in salt solution) aptamer layer on the surface.[12] From both the perspective of electrostatic and steric stabilization, folded ap-

tamers are more extended from the surface and therefore have a higher stabilization effect on AuNPs than unfolded aptamers.

In noncrosslinking aggregation systems, van der Waals attraction dominates aggregation once interparticle repulsive forces are insufficient to stabilize AuNPs. The loss of colloidal stabilization, often modulated by salt, can be realized by removing surface charges and surface-grafted (charged) polymers, and by target-induced (charged) polymer conformational transitions. The mechanism of AuNP aggregation induced by the loss of colloidal stabilizers in pathways G and H is relatively simple to interpret. In contrast, AuNP aggregation that results from (charged) polymer conformational changes on AuNP surfaces (pathway I) is more complex. Many parameters, including surface charge properties (e.g., charge density, the amount of associated counter ions) and entropy factors are involved in these systems. This can make such systems case-specific, and the general rules for the design of such assays can only be obtained with a full understanding of the effects of (charged) polymer conformations on colloidal stability and aggregation.

Compared to interparticle crosslinking aggregation systems, the noncrosslinking aggregation mechanism has some attractive features. First, neither interparticle biorecognition nor a target analyte/receptor that bears multiple binding sites is required. Moreover, aggregation induced by the noncrosslinking process is very rapid and assays can often be completed in a few minutes. This is presumably due to the nature of noncrosslinking aggregation. Once the interparticle repulsive forces are significantly reduced, the interparticle attractive forces (van der Waals) dominate and result in rapid aggregation.[12,21a] Nevertheless, as salts are often used to modulate AuNP stability and aggregation in noncrosslinking aggregation systems, one might need to choose the proper salt type and concentration in order to achieve optimal assay performance. In cases in which biomolecular functions are not compatible with certain salt types and/or concentrations, one might need to either choose a salt that has no effect on the biomolecular activity or seek a compromise between biomolecular performance and AuNP stability/aggregation at a specific salt concentration.[23b]

It is worth noting that the classification of the aggregation mechanisms into "interparticle crosslinking" and "noncrosslinking", and the definitions of each platform (pathways A–I) in these two categories are rather arbitrary. There can be an interplay between these two aggregation mechanisms. One could even design assays in which colloid aggregation is induced by a combination of factors in interparticle crosslinking and noncrosslinking aggregation mechanisms. For instance, Bhatia and co-workers prepared two types of colloidal magnetic particles (although not AuNPs) that were modified by either avidin or biotin.[26a] These two types of particles aggregate upon mixing due to interparticle avidin–biotin biorecognition. To avoid such aggregation, these particles were further modified by peptide-tethered polyethylene glycol (PEG). Avidin–biotin interaction was then prohibited by the steric hindrance provided by the PEG layers. The addition of a protease that cleaved the peptide linker and therefore removed the PEG layers (i.e., the colloidal stabilizer was removed—a strategy often used in noncrosslinking aggregation) allowed avidin to interact with biotin; this resulted in the aggregation of particles (interparticle crosslinking). This example clearly demonstrates the versatility of controlling colloidal stability and aggregation by defining interparticle forces associated with both interparticle crosslinking and noncrosslinking aggregation mechanisms.

6. Conclusion and Outlook

We have summarized recent advances in the development of AuNP-based colorimetric biosensing assays that employ interparticle plasmon coupling. The key in these assays is to control AuNP aggregation and dispersion stages that are guided by interparticle attractive and repulsive forces. Colloidal parameters, such as surface charges (charge amount and density) and surface grafted polymers (molecular weight, graft density and conformations) are important for both interparticle crosslinking and noncrosslinking aggregation mechanisms.

While our aim is to provide a general guidance for the design of AuNP absorption-based colorimetric biosensing assays, we also hope that the strategies of controlling colloidal aggregation/dispersion discussed herein can be applied in other AuNP-based sensing platforms, such as plasmonic light scattering[3b] and SERS,[3c–e] which exploit interparticle interactions, and other colorimetric assays in which a red color is developed during the growth of AuNPs triggered by a target biological process.[26b,c] We also hope that these principles can facilitate research in nanoassembly fields for the construction of well-defined nanostructures by assembling AuNPs or other types of nanoscale materials (e.g., quantum dots, nanotubes, nanowires).

Given that AuNP-based colorimetric assays are compatible with some practical platforms, for example microfluidic devices, dipstick-type assays, and other solid substrates,[27] the development of such new devices represents one future direction of AuNP-based colorimetric probes. We are currently examining such feasibilities using paper-based substrates.[28] We have found that the colors and color changes of AuNPs and their aggregation/dispersion properties are maintained on (or in) paper-based substrates. Therefore, the combination of AuNPs and paper-based substrates[29] could provide opportunities for cheap, low-volume, portable, disposable, and easy-to-use bioassay development.

AuNP-based colorimetric assays can also be used as an indirect yet simple tool to complement other techniques, such as NMR, X-ray crystallography, and to interpret biomolecular behavior (e.g., conformational changes) on surfaces, provided that such conformational changes modify AuNP colloidal stabilities and lead to different AuNP colors upon aggregation/dispersion. This is the case in which the binding of a ssDNA probe (or DNA aptamer) to its complementary DNA target (or non-nucleic acid target) on AuNP surface causes a significant colloidal stability change.[12,21] Similar assays could be used to interpret other DNA (or RNA) structures (e.g., triplex, G quadruplex, hairpin, i motif) and protein structures (particularly their conformational transitions).[19b,30] The study of such systems would not only facilitate our understanding of the biological

functions of these biomolecules, but also provide guidance for the development of surface-based biosensing devices (e.g., microarrays and nanoparticles). Furthermore, the new discoveries in these studies would also complement the traditional theories in colloidal and polymer chemistry.

Acknowledgements

We thank Prof. Qiyin Fang for helpful discussions on the physical properties of AuNPs. This work was supported by Natural Sciences and Engineering Research Council of Canada (NSERC), Sentinel Bioactive Paper Network. Y.L. holds a Canada Research Chair.

Keywords: biosensors · colloids · gold · nanotechnology · surface plasmon resonance

[1] a) S. K. Ghosh, T. Pal, *Chem. Rev.* **2007**, *107*, 4797–4862; b) M.-C. Daniel, D. Astruc, *Chem. Rev.* **2004**, *104*, 293–346; c) R. Baron, B. Willner, I. Willner, *Chem. Commun.* **2007**, 323–332; d) E. Katz, I. Willner, *Angew. Chem.* **2004**, *116*, 6166–6235; *Angew. Chem. Int. Ed.* **2004**, *43*, 6042–6108; e) N. L. Rosi, C. A. Mirkin, *Chem. Rev.* **2005**, *105*, 1547–1562; f) J. J. Storhoff, C. A. Mirkin, *Chem. Rev.* **1999**, *99*, 1849–1862; g) C. S. Thaxton, D. G. Georganopoulou, C. A. Mirkin, *Clin. Chim. Acta* **2006**, *363*, 120–126; h) Y. Lu, J. Liu, *Acc. Chem. Res.* **2007**, *40*, 315–323; i) C. M. Niemeyer, U. Simon, *Eur. J. Inorg. Chem.* **2005**, 3641; j) M. Hu, J. Chen, Z. Li, L. Au, G. V. Hartland, X. Li, M. Marqueze, Y. Xia, *Chem. Soc. Rev.* **2006**, *35*, 1084–1094; k) K. Sato, K. Hosokawa, M. Maeda, *Anal. Sci.* **2007**, *23*, 17–20; l) T. Pellegrino, S. Kudera, T. Liedl, J. A. Muñoz, L. Manna, W. J. Parak, *Small* **2005**, *1*, 48–63.

[2] a) S. Link, M. A. El-Sayed, *Annu. Rev. Phys. Chem.* **2003**, *54*, 331–366; b) S. Link, M. A. El-Sayed, *J. Phys. Chem. B* **1999**, *103*, 8410–8426.

[3] a) J. H. Teichroeb, J. A. Forrest , V. Ngai, L. W. Jones, *Eur. Phys. J. E.* **2006**, *21*, 19–24; b) K. Aslan, J. R. Lakowicz, C. D. Geddes, *Curr. Opin. Chem. Biol.* **2005**, *9*, 538–544; c) R. F. Aroca, R. A. Alvarez-Puebla, N. Pieczonka, S. Sanchez-Cortez, J. V. Garcia-Ramos, *Adv. Colloid. Interface. Sci.* **2005**, *116*, 45–61; d) M. Y. Sha, H. Xu, S. G. Penn, R. Cromer, *Nanomedicine* **2007**, *2*, 725–734; e) K. Kneipp, H. Kneipp, J. Kneipp, *Acc. Chem. Res.* **2006**, *39*, 443–450; f) C. D. Geddes, J. R. Lakowicz, *J. Fluoresc.* **2002**, *12*, 121–129; g) B. Dubertret, M. Calame, A. J. Libchaber, *Nat. Biotechnol.* **2001**, *19*, 365–370; h) D. J. Maxwell, J. R. Taylor, S. Nie, *J. Am. Chem. Soc.* **2002**, *124*, 9606–9612; i) L. Authier, C. Grossiord, P. Brossier, B. Limoges, *Anal. Chem.* **2001**, *73*, 4450–4456; j) M. Ozsoz, A. Erdem, K. Kerman, D. Ozkan, B. Tugrul, N. Topcuoglu, H. Ekren, M. Talyan, *Anal. Chem.* **2003**, *75*, 2181–2187; k) M. T. Castañeda, S. Alegret, A. Merkoçi, *Electroanalysis* **2007**, *19*, 743–753; l) R. Lévy, N. T. K. Thanh, R. C. Doty, I. Hussain, R. J. Nichols, D. J. Schiffrin, M. Brust, D. G. Fernig, *J. Am. Chem. Soc.* **2004**, *126*, 10076–10084.

[4] G. Mie, *Ann. Phys.* **1908**, *330*, 377–445.

[5] R. Elghanian, J. J. Storhoff, R. C. Mucic, R. L. Letsinger, C. A. Mirkin, *Science* **1997**, *277*, 1078–1081.

[6] a) S. Guo, E. Wang, *Anal. Chim. Acta* **2007**, *598*, 181–192; b) E. Hutter, J. H. Fendler, *Adv. Mater.* **2004**, *16*, 1685–1706.

[7] a) C. Lin, Y. Liu, S. Rinker, H. Yan, *ChemPhysChem* **2006**, *7*, 1641–1647; b) Z. Deng, S. H. Lee, C. Mao, *J. Nanosci. Nanotechnol.* **2005**, *5*, 1954–1963; c) N. C. Seeman, *Nature* **2003**, *421*, 427; d) K. V. Gothelf, T. H. LaBean, *Org. Biomol. Chem.* **2005**, *3*, 4023–4037.

[8] a) N. K. Navani, Y. Li, *Curr. Opin. Chem. Biol.* **2006**, *10*, 272–281; b) Y. Lu, J. Liu, *Curr. Opin. Biotechnol.* **2006**, *17*, 580–588; c) D. A. Schultz, *Curr. Opin. Biotechnol.* **2003**, *14*, 13–22; d) S. G. Penn, L. He, M. J. Natan, *Curr. Opin. Chem. Biol.* **2003**, *7*, 609–615; e) N. Nath, A. Chilkoti, *J. Fluoresc.* **2004**, *14*, 377–389.

[9] a) D. H. Napper, *Polymeric Stabilization of Collodial Dispersions*; Academic Press, London, **1983**; b) C. L. De Vasconcelos, M. R. Pereira, J. L. C. Fonseca, *J. Dispersion Sci. Technol.* **2005**, *26*, 59–70; c) R. J. Hunter, *Foundations of Colloid Science*; Oxford University Press, New York, **2004**; d) D. F. Evans, H. Wennerström, *The Colloidal Domain: Where Physics, Chemistry, Biology and Technology Meet*, 2nd ed., Wiley-VCH, Weinheim, **1999**; e) W. R. J. Glomm, *J. Dispersion Sci. Technol.* **2005**, *26*, 389–414; f) H. W. Walker, S. B. Grant, *Langmuir* **1996**, *12*, 3151–3156.

[10] J. Turkevich, P. C. Stevenson, J. Hillier, *Discuss. Faraday Soc.* **1951**, *11*, 55–75.

[11] W. Zhao, W. Chiuman, J. Lam, M. A. Brook, Y. Li, *Chem. Commun.* **2007**, 3729–3731.

[12] W. Zhao, W. Chiuman, J. Lam, S. A. McManus, W. Chen, Y. Cui, R. Pelton, M. A. Brook, Y. Li, *J. Am. Chem. Soc.* **2008**, *130*, 3610–3618.

[13] a) J. Lee, P. A. Ulmann, M. Han, C. A. Mirkin, *Nano Lett.* **2008**, *8*, 529–533; b) M. Han, A. K. R. Lytton-Jean, C. A. Mirkin, *J. Am. Chem. Soc.* **2006**, *128*, 4954–4955; c) J. Lee, M. Han, C. A. Mirkin, *Angew. Chem.* **2007**, *119*, 4171–4174; *Angew. Chem. Int. Ed.* **2007**, *46*, 4093–4096; d) M. Han, A. K. R. Lytton-Jean, B. Oh, J. Heo, C. A. Mirkin, *Angew. Chem.* **2006**, *118*, 1839–1842; *Angew. Chem. Int. Ed.* **2006**, *45*, 1807–1810; e) S. J. Hurst, M. Han, A. K. R. Lytton-Jean, C. A. Mirkin, *Anal. Chem.* **2007**, *79*, 7201–7205.

[14] a) V. Pavlov, Y. Xiao, B. Shlyahovsky, I. Willner, *J. Am. Chem. Soc.* **2004**, *126*, 11768–11769; b) C. C. Huang, Y. F. Huang, Z. Cao, W. Tan, H. T. Chang, *Anal. Chem.* **2005**, *77*, 5735–5741; c) Y. Huang, H. Chang, *Anal. Chem.* **2007**, *79*, 4852–4859; d) C. Wang, Y. Chen, T. Wang, Z. Ma, Z. Su, *Chem. Mater.* **2007**, *19*, 5809–5811; e) A. Gole, C. J. Murphy, *Langmuir* **2005**, *21*, 10756–10762; f) N. Thanh, Z. Rosenzweig, *Anal. Chem.* **2002**, *74*, 1624–1628; g) Z. Wu, M. Guo, G. Shen, R. Yu, *Anal. Bioanal. Chem.* **2007**, *387*, 2623–2626; h) C. L. Schofield, R. A. Field, D. A. Russell, *Anal. Chem.* **2007**, *79*, 1356–1361; i) Y. Kim, R. C. Johnson, J. T. Hupp, *Nano Lett.* **2001**, *1*, 165–167; j) C. D. Medley, J. E. Smith, Z. Tang, Y. Wu, S. Bamrungsap, W. Tan, *Anal. Chem.* **2008**, *80*, 1067–1072; k) X. Xue, F. Wang, X. Liu, *J. Am. Chem. Soc.* **2008**, *130*, 3244–3245; l) F. Seela, S. Budow, *Helv. Chim. Acta* **2006**, *89*, 1978–1985; m) G. R. Souza, D. R. Christianson, F. I. Staquicini, M. G. Ozawa, E. Y. Snyder, R. L. Sidman, J. H. Miller, W. Arap, R. Pasqualini, *Proc. Nat. Acad. Sci. USA* **2006**, *103*, 1215–1220; n) S. Connolly, D. Fitzmaurice, *Adv. Mater.* **1999**, *11*, 1202–1205; o) H. Otsuka, Y. Akiyama, Y. Nagasaki, K. Kataoka, *J. Am. Chem. Soc.* **2001**, *123*, 8226–8230; p) D. C. Hone, A. H. Haines, D. A. Russell, *Langmuir* **2003**, *19*, 7141–7144; q) P. K. Sudeep, S. T. S. Joseph, K. G. Thomas, *J. Am. Chem. Soc.* **2005**, *127*, 6516–6517; r) P. Hazarika, B. Ceyhan, C. M. Niemeyer, *Small* **2005**, *1*, 844–848; s) G. Song, C. Chen, X. Qu, D. Miyoshi, J. Ren, N. Sugimoto, *Adv. Mater.* **2008**, *20*, 706–710; t) M. K. Beissenhirtz, R. Elnathan, Y. Weizmann, I. Willner, *Small* **2007**, *3*, 375–379; u) W. Yang, J. J. Gooding, Z. He, Q. Li, G. Chen, *J. Nanosci. Nanotechnol.* **2007**, *7*, 712–716; v) J. Nam, A. R. Wise, J. T. Groves, *Anal. Chem.* **2005**, *77*, 6985–6988.

[15] a) J. Liu, Y. Lu, *J. Am. Chem. Soc.* **2005**, *127*, 12677–12683; b) J. Liu, Y. Lu, *Angew. Chem.* **2006**, *118*, 8123–8127; *Angew. Chem. Int. Ed.* **2006**, *45*, 90–94; c) J. Liu, Y. Lu, *Org. Biomol. Chem.* **2006**, *4*, 3435–3441; d) J. Liu, Y. Lu, *Adv. Mater.* **2006**, *18*, 1667–1671.

[16] a) K. Aslan, J. R. Lakowicz, C. D. Geddes, *Anal. Chim. Acta* **2004**, *517*, 139–144; b) K. Aslan, J. R. Lakowicz, C. D. Geddes, *Anal. Biochem.* **2004**, *330*, 145–155.

[17] C. Tsai, T. Yu, C. Chen, *Chem. Commun.* **2005**, 4273–4275.

[18] a) C. Guarise, L. Pasquato, V. De Filippis, P. Scrimin, *Proc. Natl. Acad. Sci. USA* **2006**, *103*, 3978–3982; b) Y. Choi, N. Ho, C. Tung, *Angew. Chem.* **2007**, *119*, 721–723; *Angew. Chem. Int. Ed.* **2007**, *46*, 707–709; c) Z. Wu, S. Zhang, M. Guo, C. Chen, G. Shen, R. Yu, *Anal. Chim. Acta* **2007**, *584*, 122–128; d) R. Liu, R. Liew, J. Zhou, B. Xing, *Angew. Chem.* **2007**, *119*, 2069–2073; *Angew. Chem. Int. Ed.* **2007**, *46*, 2023–2027; e) A. T. Gates, S. O. Fakayode, M. Lowry, G. M. Ganea, A. Murugeshu, J. W. Robinson, R. M. Strongin, I. M. Warner, *Langmuir* **2008**, *24*, 4107–4113; f) J. Liu, Y. Lu, *J. Am. Chem. Soc.* **2003**, *125*, 6642–6643; g) J. Liu, Y. Lu, *Anal. Chem.* **2004**, *76*, 1627–1632; h) J. Liu, Y. Lu, *Chem. Commun.* **2007**, 4872–4874.

[19] a) Z. Wang, R. Lévy, D. G. Fernig, M. Brust, *J. Am. Chem. Soc.* **2006**, *128*, 2214–2215; b) S. Chah, M. R. Hammond, R. Zare, *Chem. Biol.* **2005**, *12*, 323–328; c) J. Sharma, R. Chhabra, H. Yan, Y. Liu, *Chem. Commun.* **2007**, 477–479; d) W. Wang, H. Liu, D. Liu, Y. Xu, Y. Yang, D. Zhou, *Langmuir* **2007**, *23*, 11956–11959.

[20] a) X. Xu, M. Han, C. A. Mirkin, *Angew. Chem.* **2007**, *119*, 3538–3540; *Angew. Chem. Int. Ed.* **2007**, *46*, 3468–3470; b) A. Laromaine, L. Koh, M. Murugesan, R. V. Ulijn, M. M. Stevens, *J. Am. Chem. Soc.* **2007**, *129*, 4156–4157; c) K. Aslan, C. C. Luhrs, V. H. Pérez-Luna, *J. Phys. Chem. B* **2004**, *108*, 15631–15639.

[21] a) K. Sato, K. Hosokawa, M. Maeda, *J. Am. Chem. Soc.* **2003**, *125*, 8102–8103; b) D. Miyamoto, Z. Tang, T. Takarada, M. Maeda, *Chem. Commun.*

2007, 4743–4745; c) Y. Sato, K. Hosokawa, M. Maeda, *Colloids Surf. B* **2008**, *62*, 71–76; d) K. Sato, M. Onoguchi, Y. Sato, K. Hosokawa, M. Maeda, *Anal. Biochem.* **2006**, *350*, 162–164; e) K. Sato, K. Hosokawa, M. Maeda, *Nucleic Acids Res.* **2005**, *33*, e4.

[22] a) H. Li, L. J. Rothberg, *Proc. Nat. Acad. Sci. USA* **2004**, *101*, 14036–14039; b) H. Li, L. J. Rothberg, *J. Am. Chem. Soc.* **2004**, *126*, 10958–10961; c) H. Li, L. J. Rothberg, *Anal. Chem.* **2005**, *77*, 6229–6233; d) L. Wang, X. Liu, X. Hu, S. Songa, C. Fan, *Chem. Commun.* **2006**, 3780–3782; e) H. Wei, B. Li, J. Li, E. Wang, S. Dong, *Chem. Commun.* **2007**, 3735–3737; f) J. Wang, L. Wang, X. Liu, Z. Liang, S. Song, W. Li, G. Li, C. Fan, *Adv. Mater.* **2007**, *19*, 3943–3946; g) J. Oishi, Y. Asami, T. Mori, J. Kang, M. Tanabe, T. Niidome, Y. Katayama, *ChemBioChem* **2007**, *8*, 875–879; h) J. Oishi, X. Han, J. Kang, Y. Asami, T. Mori, T. Niidome, Y. Katayama, *Anal. Biochem.* **2008**, *373*, 161–163; i) Y. M. Chen, C. J. Yu, T. L. Cheng, W. L. Tseng, *Langmuir* **2008**, *24*, 3654–3660; j) D. Li, A. Wieckowska, I. Willner. *Angew. Chem.* **2008**, *120, 3991–3995; Angew. Chem. Int. Ed.* **2008**, 47, 3927–3931; *Angew. Chem. Int. Ed.* **2008**, *47*, 3927–3931.

[23] a) W. Zhao, W. Chiuman, M. A. Brook, Y. Li, *ChemBioChem* **2007**, *8*, 727–731; b) W. Zhao, J. Lam, W. Chiuman, M. A. Brook, Y. Li, *Small* **2008**, *4*, 810–816.

[24] a) R. Nutiu, Y. Li, *Methods* **2005**, *37*, 16–25; b) R. Nutiu, J. M. Yu, Y. Li, *ChemBioChem* **2004**, *5*, 1139–1144; c) R. Nutiu, Y. Li, *Chem. Eur. J.* **2004**, *10*, 1868–1876; d) R. Nutiu, Y. Li, *J. Am. Chem. Soc.* **2003**, *125*, 4771–4778.

[25] a) S. W. Santoro, G. F. Joyce, *Proc. Natl. Acad. Sci. USA* **1997**, *94*, 4262–4266; b) J. Li, Y. Lu, *J. Am. Chem. Soc.* **2000**, *122*, 10466–10467.

[26] a) G. von Maltzahn, T. J. Harris, J. Park, D. Min, A. J. Schmidt, M. J. Sailor, S. N. Bhatia, *J. Am. Chem. Soc.* **2007**, *129*, 6064–6065; b) R. Baron, M. Zayats, I. Willner, *Anal. Chem.* **2005**, *77*, 1566–1571; c) M. Zayats, R. Baron, I. Popov, I. Willner, *Nano Lett.* **2005**, *5*, 21–25.

[27] a) J. Liu, D. Mazumdar, Y. Lu, *Angew. Chem.* **2006**, *118*, 8123–8127; *Angew. Chem. Int. Ed.* **2006**, *45*, 7955–7959; b) K. Glynou, P. C. Ioannou, T. K. Christopoulos, V. Syriopoulou, *Anal. Chem.* **2003**, *75*, 4155–4160; c) I. K. Litos, P. C. Ioannou, T. K. Christopoulos, J. Traeger-Synodinos, E. Kanavakis, *Anal. Chem.* **2007**, *79*, 395–402; d) L. He, M. D. Musick, S. R. Nicewarner, F. G. Salinas, S. J. Benkovic, M. J. Natan, C. D. Keating, *J. Am. Chem. Soc.* **2000**, *122*, 9071–9077.

[28] a) Sentinel Bioactive Paper: http://www.bioactivepaper.ca/; b) W. Zhao, M. M. Ali, S. D. Aguirre, M. A. Brook, Y. Li, *Anal. Chem.* **2008**, in press.

[29] A. W. Martinez, S. T. Phillips, M. J. Butte, G. M. Whitesides, *Angew. Chem.* **2007**, *119*, 1340–1342; *Angew. Chem. Int. Ed.* **2007**, *46*, 1318–1320.

[30] D. Murphy, R. Eritja, G. Redmond, *Nucleic Acids Res.* **2004**, *32*, e65.

[31] a) P. Baptista, E. Pereira, P. Eaton, G. Doria, A. Miranda, I. Gomes, P. Quaresma, R. Franco, *Anal. Bioanal. Chem.* **2008**, *391*, 943–950; b) P. V. Baptista, M. Koziol-Montewka, J. Paluch-Oles, G. Doria, R. Franco, *Clin. Chem.* **2006**, *52*, 1433–1434; c) P. Baptista, G. Doria, D. Henriques, E. Pereira, R. Franco, *J. Biotechnol.* **2005**, *119*, 111–117.

Received: April 24, 2008
Published online on September 26, 2008

